

See discussions, stats, and author profiles for this publication at: <https://www.researchgate.net/publication/228420824>

Two-Photon Excitation of Fluorogenic Probes for Redox Metabolism: Dramatic Enhancement of Optical Contrast Ratio by Two-Photon Excitation

ARTICLE *in* THE JOURNAL OF PHYSICAL CHEMISTRY C · JUNE 2007

Impact Factor: 4.77 · DOI: 10.1021/jp067430h

CITATIONS

10

READS

13

10 AUTHORS, INCLUDING:



[Steffen Jockusch](#)

Columbia University

220 PUBLICATIONS 6,209 CITATIONS

SEE PROFILE



[Qingdong Zheng](#)

Chinese Academy of Sciences

82 PUBLICATIONS 2,918 CITATIONS

SEE PROFILE

Two-Photon Excitation of Fluorogenic Probes for Redox Metabolism: Dramatic Enhancement of Optical Contrast Ratio by Two-Photon Excitation[†]

Steffen Jockusch,[‡] Qingdong Zheng,[§] Guang S. He,[§] Haridas E. Pudavar,[§] Dominic J. Yee,[‡] Vojtech Balsanek,[‡] Marlin Halim,[‡] Dalibor Sames,^{*,‡} Paras N. Prasad,[§] and Nicholas J. Turro^{*,‡}

Department of Chemistry, Columbia University, 3000 Broadway, New York, New York 10027, and Institute for Lasers, Photonics and Biophotonics, and Department of Chemistry, State University of New York at Buffalo, Buffalo, New York 14260

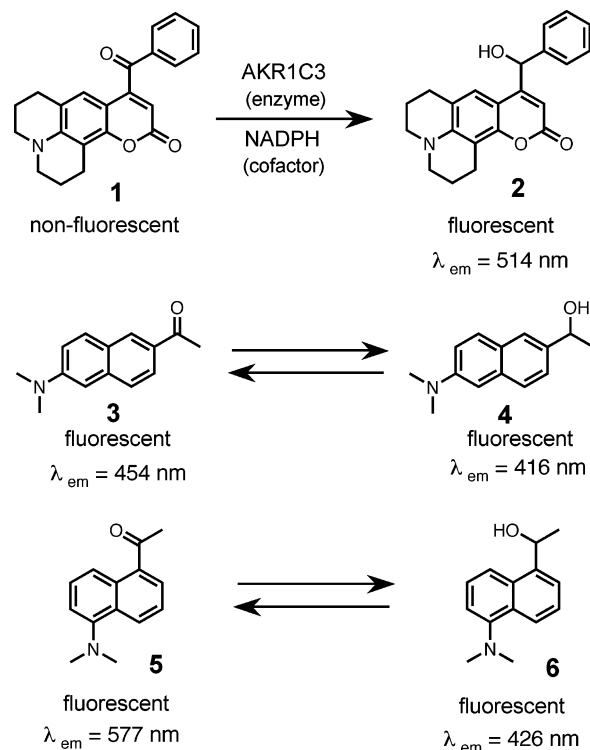
Received: November 9, 2006; In Final Form: February 15, 2007

Fluorogenic probes for redox metabolism are shown to exhibit two-photon absorption using femtosecond pulses from a Ti:sapphire laser. The probes consist of a coumarin or naphthalene core and a ketone–alcohol functional group. The probe design is based on the changes in fluorescence properties and two-photon cross section values when the ketone derivative is reduced to the corresponding alcohol. The resulting contrast ratio of the fluorescence differs significantly from that obtained by one-photon excitation. This phenomenon was demonstrated with all three switches examined herein and represents an attractive approach to modulation of emission properties of molecular switches. The practical applicability of the two-photon-excitation redox switch was demonstrated in an enzyme-catalyzed transformation. The nonfluorescent probe **1** is efficiently converted by AKR1C3, a human 3 α -hydroxysteroid dehydrogenase, to the fluorescent derivative **2**. Using two-photon excitation (775 nm), we achieved a large contrast ratio between the fluorescence in the presence and the absence of the enzyme of ~ 300 .

Introduction

Molecular imaging of metabolic and signaling events in living systems represents an important frontier in modern chemical biology.¹ Molecular optical imaging can benefit from the generation of “smart” probes or functional dyes^{2,3} which provide an optical signal for a particular enzyme facilitated molecular process.^{4,5} Fluorogenic probes have been reported which are selective for 3 α -hydroxysteroid dehydrogenases (3 α -HSD), an important class of enzymes in human physiology (steroid metabolism, stress response).^{6,7} Some of the most promising fluorogenic probes are designed as ketone–alcohol redox switches, where the probe is a competitive substrate to the enzyme.^{6,7} As an example, Scheme 1 shows a coumarin pair, where the virtually nonfluorescent ($\Phi_f < 0.001$) ketone derivative (**1**) is reduced by the human 3 α -HSD enzyme (AKR1C3) in the presence of protein cofactor NADPH to the alcohol derivative (**2**), which is strongly fluorescent ($\Phi_f = 0.65$). However, a major disadvantage of these ketone–alcohol fluorogenic probes is the short excitation wavelength (UV) which is necessary to excite these chromophores. Short excitation wavelengths possess only a minimal penetration depth in tissue, show increased light scattering, promote tissue autofluorescence, and damage tissues. These disadvantages limit the application of the ketone–alcohol fluorogenic probes in microscopy imaging of living cells, tissues, and organisms. On the other hand, two-photon absorption (simultaneous absorption of two photons of near-infrared, NIR, light) has been demonstrated to overcome the problems of short-wavelength excitation for many applica-

SCHEME 1: Structure of the Investigated Ketone–Alcohol Redox Probes and Fluorescence Maxima in Aqueous Buffer (2) Acetonitrile (3–6) Solutions



[†] Part of the special issue “Kenneth B. Eisenthal Festschrift”.

* Corresponding authors. E-mail: njt3@columbia.edu (N.J.T.) and sames@chem.columbia.edu (D.S.).

[‡] Columbia University.

[§] State University of New York at Buffalo.

tions.^{8–10} Two-photon absorption is gaining interest in a number of interdisciplinary areas, such as fluorescence imaging, phototherapy, and biophotonics because of its advantages over traditional one-photon absorption. For two-photon absorption,

NIR laser light can be used, which allows deep penetration into biological targets such as tissue and organs. In addition, in fluorescence detection methods, a low background is achieved because of the large spectral separation of excitation light and fluorescence emission signal, which allows the use of wideband filters for fluorescence detection. Also, autofluorescence is significantly reduced because two-photon absorption shows a quadratic dependence on the excitation light intensity; focused light beams are often used, which makes spatial isolation of the excitation event possible and increases the depth resolution in microscopy. In addition, damage to the biological systems is reduced by using NIR light compared with traditional UV excitation.

Experimental Section

Materials. The synthesis of the probes **1–6** (Scheme 1) have been described previously.^{6,7} Human aldo-keto reductase, AKR1C3 (type 2 3 α -hydroxysteroid dehydrogenase/type 5 17 β -hydroxysteroid dehydrogenase) was a generous gift of Professor Trevor M. Penning (University of Pennsylvania School of Medicine). Enzyme cofactor NADPH was purchased from Roche.

Methods. UV–vis absorption spectra were recorded on an Agilent 8453 spectrophotometer using quartz cells with a path length of 10 mm.

Fluorescence Quantum Yield Determination. Fluorescence emission spectra for fluorescence quantum yield determination were recorded at room temperature on a SPEX Fluorolog-3 spectrometer FL3–22 (J. Y. Horiba, Edison, NJ) using quartz cells with a path length of 10 mm. 9,10-Diphenylanthracene was used as the fluorescence standard ($\phi_f = 0.95$).¹¹

Two-Photon Excited Fluorescence. As an excitation source, a Ti:sapphire laser oscillator/amplifier system (CPA-2010 from Clark-MXR) was used, which generated pulses at ~ 775 nm (~ 8 nm spectral width) with a pulse duration of ~ 150 fs at a repetition rate of 1 kHz. The laser beam was focused by an $f = 20$ cm lens, and the sample cell (1×1 cm quartz cuvette) was placed at a distance of ~ 22 cm from the focusing lens. The fluorescence of the sample was collected at 90° from the excitation light by using a HoloSpec CCD-array spectrometer in conjunction with a fiber coupler head.

Two-Photon Cross Section Determination by a Nonlinear Transmission Method. The two-photon absorption cross section (δ) of **2** was determined by using the pulses (~ 775 nm, ~ 150 fs duration, 1 kHz repetition rate, $6 \mu\text{J/pulse}$) from a Ti:sapphire laser oscillator/amplifier system (CPA-2010 from Clark-MXR) by measuring the nonlinear transmissivity of the sample solution and standard solution as a function of the input light intensity.¹² The nonlinear transmission T depends on the input IR laser intensity I_0 , and can be written as

$$T(I_0) = [\ln(1 + I_0\beta l)]/(I_0\beta l) \quad (1)$$

where l is the optical path length of the sample, β is two-photon absorption coefficient of the sample solution and can be experimentally determined by measuring the T value at a given I_0 level. Knowing the β value (in units of cm^2/W) for a sample, we can further determine the molecular two-photon absorption cross-section δ (in units of $\text{cm}^4\cdot\text{s}/\text{photon}$) according to the following relationship:

$$\delta = h\nu\beta/(N_A d_0 \times 10^{-3}) \quad (2)$$

where N_A is the Avogadro number, d_0 is the molar concentration of the dye solution, and $h\nu$ is the energy of an incident photon.

Absolute values of two-photon cross sections are very difficult to measure, mostly because of the difficulty in determination of I_0 , the peak intensity of the laser pulse. Furthermore, the temporal and spatial laser beam profile often deviates from the ideal condition. Therefore, a relative method was used to determine the two-photon cross section values employing the standard AF-350 ($\delta = 206 \text{ GM}$ at 775 nm in tetrahydrofuran, THF).¹³ First, the nonlinear transmission, T_{standard} of the standard was measured. Using eq 2, the β_{standard} value was determined. The value of T_{sample} of the sample was measured under identical excitation conditions. Knowing T_{standard} , β_{standard} , and T_{sample} , we can calculate the value of β_{sample} using eq 1. With the value of β_{sample} , the two-photon cross section (δ_{sample}) was calculated using eq 2.

Two-Photon Cross Section Spectra from Two-Photon Excited Emission Spectra. A mode locked Ti:sapphire laser (Mira from Coherent) pumped by a DPSS laser (Verdi from Coherent) was used as the excitation source and generated pulses (~ 120 fs duration, 76 MHz repetition rate, $\sim 2 \text{ nJ/pulse}$) from 715 to 940 nm. A spectrum analyzer (IST-rees) was used to monitor the excitation wavelengths. The laser beam was focused into the center of the sample solution using a 5 cm focal length lens, and the fluorescence spectra were monitored using a Jobin–Yvon Fluorolog-3 spectrometer. The total fluorescence intensity collected for the samples (**2**, 40 mM in acetonitrile) and the standard (rhodamine 6G, 100 μM in methanol) at each excitation wavelength was calculated as the area under the collected fluorescence spectrum. The two-photon cross section of rhodamine 6G (100 μM solution in methanol) reported by Albota et al.¹⁴ was used as a standard for calculating the two-photon cross section of **2**.

According to Xu and Webb,¹⁵ the total two-photon excited fluorescence intensity is given by

$$\langle F(t) \rangle = \frac{1}{2} \phi \eta_2 C \delta \frac{g_p}{f\tau} \frac{8n\langle P(t) \rangle^2}{\pi\lambda} \quad (3)$$

where $\langle F(t) \rangle$ is the total average fluorescence intensity collected, η_2 is the fluorescence quantum efficiency of the dye, ϕ is the fluorescence collection efficiency of the dye, C is the concentration of the dye in solution, δ is the two-photon excitation cross section, $g_p/f\tau$ is the degree of second-order coherence (g_p depends only on pulse shape and in this case the hyperbolic-secant which has a value of $g_p = 0.588$), n is the refractive index, and $\langle P(t) \rangle$ is the average excitation power. While using a standard sample (rhodamine 6G) with known two-photon cross section, we can ignore most of the parameters in this equation, and the δ_{new} (two-photon cross section of the unknown dye) can be reduced to:¹³

$$\delta_{\text{new}} = \frac{C_{\text{rhod}}}{C_{\text{new}}} \frac{\delta_{\text{rhod}} \eta_{\text{rhod}}}{\eta_{\text{new}}} \frac{\langle F(t) \rangle_{\text{new}} n_{\text{rhod}}}{\langle F(t) \rangle_{\text{rhod}} n_{\text{new}}} \quad (4)$$

Assuming that the fluorescence quantum efficiencies of two-photon and one-photon excitation are the same, we can calculate the two-photon cross section of the unknown sample considering the fluorescence quantum yields of the unknown sample and standard. Because solutions with high concentrations of the fluorogenic probes were used (40 mM), self-quenching could reduce the fluorescence quantum yields. To correct for the self-quenching, the fluorescence lifetimes at probe concentrations of 0.1 mM (no self-quenching expected) were compared to the fluorescence lifetimes at high concentrations (40 mM). The fluorescence lifetimes are listed in Supporting Information (Table

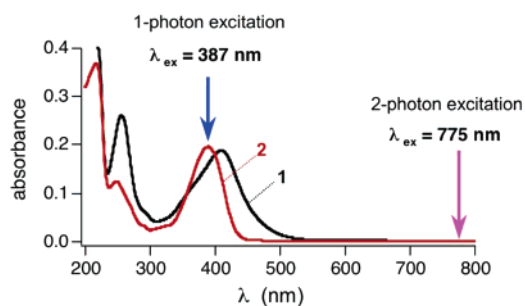


Figure 1. Absorption spectrum (one-photon absorption) of **1** (black) and **2** (red) in acetonitrile solutions. No absorbance is observed at 775 nm, the emission wavelength of the Ti:sapphire laser which we used for the two-photon excitation experiments.

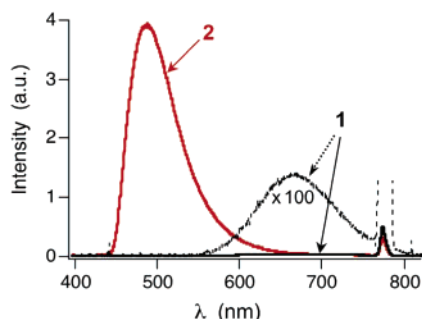


Figure 2. Fluorescence spectra of **1** (black line) and **2** (red line) in acetonitrile solutions (40 mM) after excitation with laser pulses (~ 150 fs pulse width) of 775 nm ($3.2 \mu\text{J}/\text{pulse}$). The dashed black spectrum of **1** was amplified by a factor of 100.

S2). In case of self-quenching, the fluorescence quantum yields, which were used to calculate the two-photon cross sections, were corrected on the basis of the fluorescence lifetime ratios at probe concentrations of 0.1 mM and 40 mM.

Results and Discussion

The absorbance of the ketone derivative **1** shows $\lambda_{\text{max}} = 410$ nm, whereas the fluorescent alcohol derivative **2** has a hypsochromically shifted absorption ($\lambda_{\text{max}} = 390$ nm, Figure 1). No absorbance is observed at 775 nm, which is the emission wavelength of the Ti:sapphire laser we used for the two-photon excitation experiments. Figure 2 shows the fluorescence spectra of **1** and **2** after excitation with fs laser pulses at 775 nm. A strong fluorescence of **2** was observed ($\lambda_{\text{max}} = 480$ nm). Laser power dependence studies showed that the fluorescence resulted from the two-photon absorption, because a quadratic power dependence was observed (Figure 3 right). The same fluorescence spectrum was observed after excitation in the absorption band of **2** at 387 nm (Figure 4), demonstrating that one- and two-photon absorption populate the same fluorescing excited state. Excitation of solutions containing **1** with fs laser pulses of 775 nm resulted in a very weak fluorescence of **1**, which is bathochromically shifted to **2** ($\lambda_{\text{max}} = 665$ nm, Figure 2). A quadratic laser power dependence on the fluorescence intensity was observed, indicating two-photon absorption (Figure 3). The fluorescence intensity of **2** is about 290 times more intense than that for **1**, which makes this “off–on” ketone–alcohol redox switch attractive for biological applications. Furthermore, in practical applications, such as molecular imaging of metabolism, the fluorescence intensity ratio at the fluorescence maximum of the metabolically generated fluorophore (**2**, $\lambda_{\text{max}} = 480$ nm) would be used. At 480 nm, the contrast ratio between the fluorescence intensity of **2** and that of **1** is even higher, $I_2/I_1 > 7000$ (Figure 2).

To test the practical applicability of this two-photon-excitation redox switch in an enzyme catalyzed process, the conversion of **1** into **2** catalyzed by 3 α -HSD (AKR1C3) was investigated. The 3 α -HSD enzymes are members of the aldo-keto reductase super-family and have numerous physiological functions, such as activation/deactivation of steroid hormones in various tissues.¹⁶ The fluorescence intensity at the emission maximum of **2** (514 nm, in aqueous buffer) during laser excitation at 775 nm was monitored over time for solutions containing **1**, AKR1C3, and NADPH. Figure 5 demonstrates that in the presence of both AKR1C3 and NADPH, **1** was converted into **2** (red circles), which is shown by the fluorescence buildup of **2**. However, in the absence of either AKR1C3 or NADPH, no conversion of **1** into **2** was observable by fluorescence (Figure 5, pink diamonds and blue circles, respectively). Under our experimental conditions using two-photon excitation, a large contrast ratio between the fluorescence in the presence and the fluorescence in the absence of enzyme of ~ 300 was achieved.

To further optimize the excitation wavelength for two-photon excitation, the two-photon absorption spectrum of **2** was determined as two-photon-induced fluorescence excitation spectrum. Using a tunable Ti:sapphire laser for excitation, we monitored the fluorescence intensity of **2** in comparison to the fluorescence intensity of a standard (rhodamine 6G)¹⁷ with a known two-photon absorption spectrum. The two-photon absorption spectrum of **2** shows a good overlap with the one-photon absorption spectrum (Figure 6). The optimum excitation wavelength for two-photon absorption is between 750 and 800 nm, where the two-photon cross section is maximal ($\delta = 9 \pm 1$ GM). This wavelength region matches the optimal emission output region of the currently available Ti:sapphire lasers. In addition to this fluorescence method, δ of **2** was also determined by an independent absorption method ($\delta_{775 \text{ nm}} = 4 \pm 1$ GM) in comparison to a standard with known δ .¹³ Both values for δ are in good agreement considering the different nature of the methods employed for measurement.

The naphthalene derivative pairs **3/4** and **5/6** (Scheme 1) are also good fluorescence switches and represent potential redox metabolic probes.^{6,18,19} With one-photon excitation, these naphthalene derivatives show fluorescence between 400 and 700 nm (Figure 7, right). Consistent with the expected substitution effect, the ketone derivatives, **3** and **5**, fluoresce at a longer wavelength, whereas the alcohol derivatives, **4** and **6**, fluoresce at a shorter wavelength. Therefore, these probes can be used for ratiometric analysis to monitor redox metabolism. However, the short excitation wavelength (UV spectral region) is unfavorable for practical applications. Therefore, we investigated the two-photon excitation of these naphthalene derivatives using femtosecond pulses from a Ti:sapphire laser of 775 nm. Figure 7 (left) shows fluorescence of the ketone derivatives, **3** and **5**. Interestingly, the alcohol derivatives, **4** and **6**, showed only weak fluorescence. This is opposite to what is observed for the ketone–alcohol pair of the coumarin derivative, **1** and **2**, where the alcohol derivative (**2**) shows strong fluorescence and the ketone derivative (**1**) shows only negligible fluorescence (Figure 2). High contrast ratios were observed between the fluorescence of the alcohol and that of the ketone (1:180 for **4:3** and 1:200 for **6:5**, Figure 7). Conversely, the contrast ratios for regular one-photon excitations are 2 orders of magnitude smaller (1:2.2 and 7:1, respectively). It is noteworthy that the ratio for **6:5** was reversed by moving from one-photon to two-photon excitation.

Considering the similar fluorescence quantum yields (Table 1), we find the high contrast ratios for two-photon excitation are probably caused by major differences in the two-photon

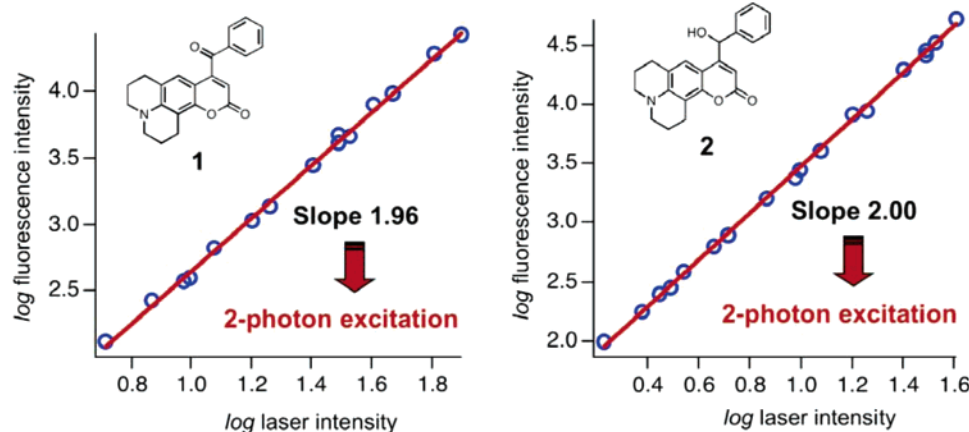


Figure 3. Fluorescence intensity of **1** (left) and **2** (right) (25 mM in acetonitrile) at 665 nm (left) and 480 nm (right) vs the laser intensity at 775 nm. The log–log plots show slopes of 1.96 and 2.00, which demonstrate two-photon absorptions.

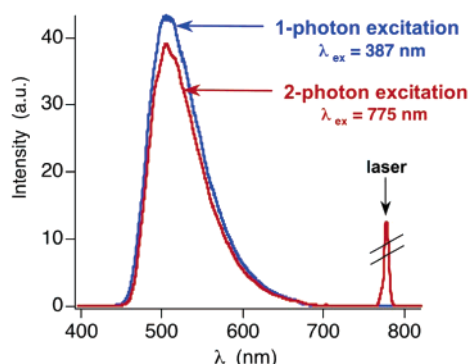


Figure 4. Fluorescence spectra of **2** after one-photon excitation (blue) and two-photon excitation (red) in aqueous solutions containing 33% acetonitrile (v/v) ($[2] = 1.8$ mM). Both fluorescence spectra are very similar demonstrating that one- and two-photon absorption populate the same fluorescing excited state.

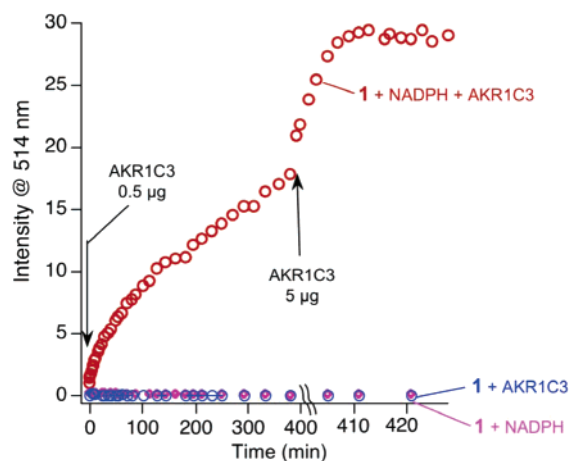


Figure 5. Enzyme catalyzed conversion of probe **1** to product **2** monitored via fluorimetry. Fluorescence intensity at 514 nm vs time after excitation with pulses (~ 150 fs pulse width) of 775 nm (3.2 μ J/pulse). The 1 mL aqueous buffer solutions (0.1 M phosphate buffer, pH = 6) contained: red circles; **1** (20 μ M), NADPH (250 μ M), and the enzyme AKR1C3 (0.5 μ g/mL), blue circles; **1** (20 μ M) and AKR1C3 (0.5 μ g/mL), and pink diamonds; **1** (20 μ M) and NADPH (250 μ M). After 400 s, another dose of AKR1C3 (5 μ g/mL) was added. Note that the displayed time scale is different after 400 s.

absorption cross sections at 775 nm. The two-photon absorption cross sections (δ) were determined by the nonlinear absorption method and by the fluorescence method as described above and are summarized in Table 1. As in agreement with the high

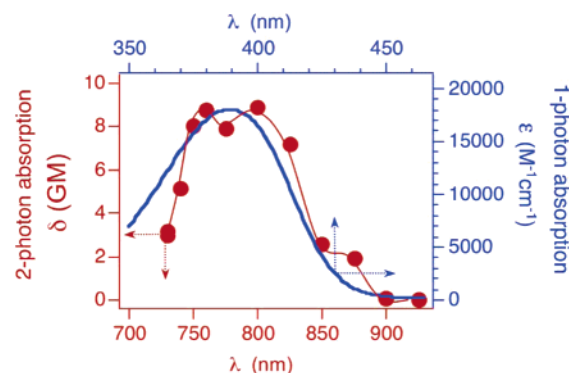


Figure 6. Two-photon (red) and one-photon (blue) absorption spectrum of **2** in acetonitrile solutions (40 mM). The two-photon absorption cross sections (δ , left axis) were determined from the two-photon-induced fluorescence excitation spectrum relative to rhodamine 6G using laser excitation (~ 120 fs pulse width; ~ 2 nJ/pulse).

contrast ratios, the δ values are significantly higher for the ketone derivatives, **3** and **5**, compared with the alcohol derivatives, **4** and **6**. Generally, high intramolecular charge separation promotes high two-photon cross section values. In the case of the ketone derivatives, **3** and **5**, the combination of the acetyl group (electron acceptor) and amino group (electron donor) on opposite ends of the molecule generates a high intramolecular charge separation. However, in the case of the alcohol derivatives, **4** and **6**, both substituents, hydroxy and amino group, are electron donors. Therefore, low intramolecular charge separation is expected, and the observed two-photon cross section values were low (Table 1). The two-photon cross sections for the alcohol derivatives, **4** and **6**, were too low to be determined with the absorption method under our experimental conditions. A discrepancy of the δ values at 775 nm excitation for **5** was observed, between the values determined by the absorption method and the fluorescence method. This discrepancy is probably caused by the low fluorescence quantum yield of **5** (Table 1).

The two-photon absorption spectra of **3–6** were determined from two-photon excitation spectra using the standard rhodamine 6G as described above. Under our experimental conditions, the maxima of two-photon absorption for **3–5** are at approximately 750 nm (Figure 8). The two-photon absorption spectrum of **6** is hypsochromically shifted compared with those of **3–5**, which is consistent with the hypsochromically shifted one-photon absorption spectrum (see Supporting Information).

To determine how many photons are absorbed simultaneously, the dependence of the intensity of the fluorescence of **3–6** on

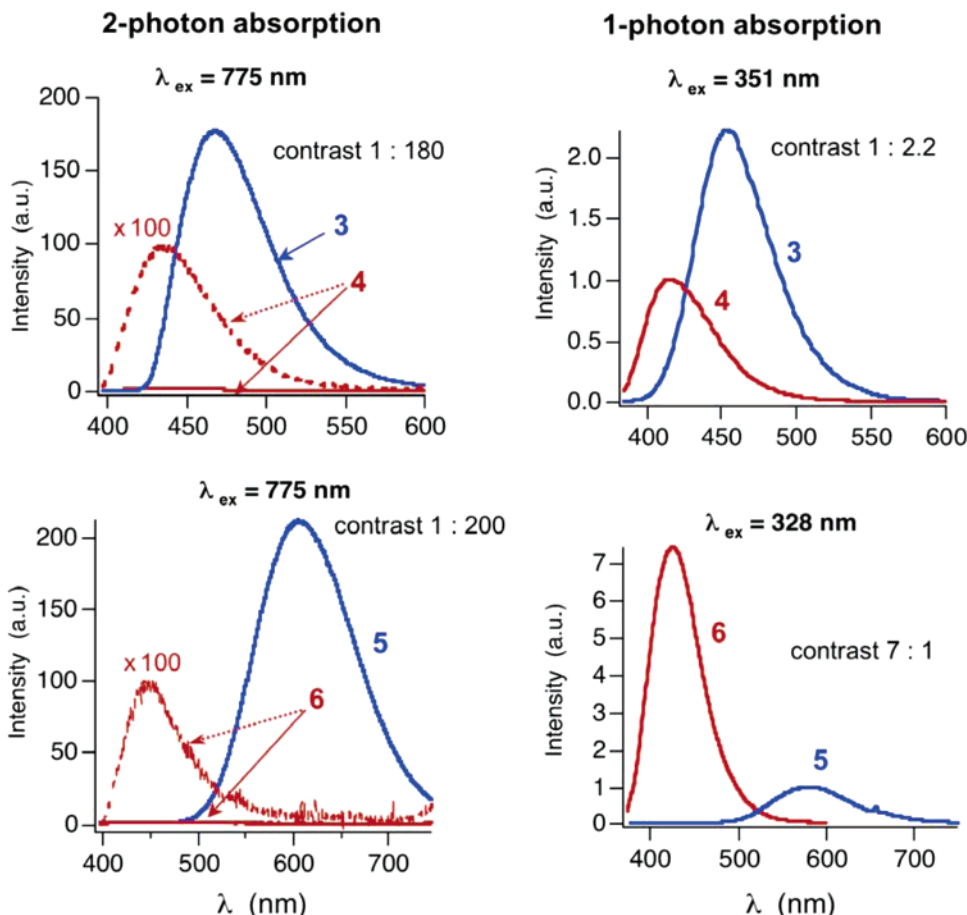


Figure 7. Left: fluorescence spectra of 3–6 in acetonitrile solutions (40 mM) after excitation with laser pulses ($\sim 150 \text{ fs}$ pulse width) of 775 nm ($3.2 \mu\text{J/pulse}$). The dashed red spectra of 4 and 6 were amplified by a factor of 100. Right: fluorescence after one-photon excitation. The contrast ratios of the fluorescence intensities at the maximum between the alcohol (red) and the ketone (blue) derivatives are given.

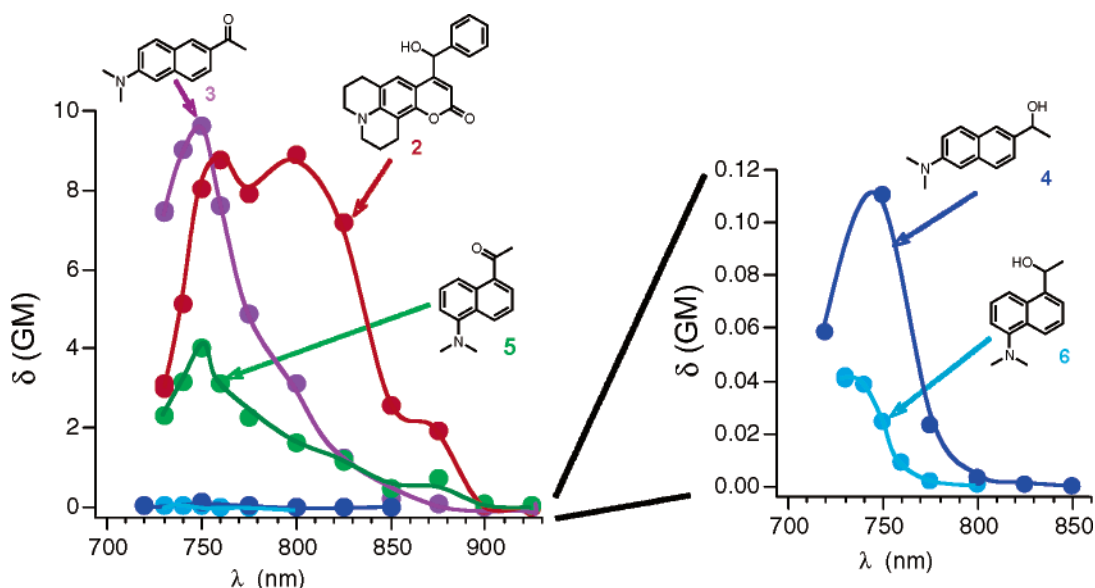


Figure 8. Two-photon absorption spectra in acetonitrile solutions (40 mM). The two-photon absorption cross sections (δ) were determined from the two-photon-induced fluorescence excitation spectra relative to rhodamine 6G using laser excitation ($\sim 120 \text{ fs}$ pulse width; $\sim 2 \text{ nJ/pulse}$).

the laser intensity of the Ti/sapphire laser at 775 nm was measured. For the naphthalene derivatives 3–5, the plots of the logarithm of the laser intensity versus the logarithm of the observed fluorescence intensities (analogous to Figure 3) showed slopes of 2.0 ± 0.05 , which indicate two-photon absorption. However, for 6, a slope of 2.3 was observed, suggesting a mixed two- and three-photon absorption at an excitation wavelength

of 775 nm. At a shorter excitation wavelength, 720 nm, a slope of 1.9 was observed, which demonstrates that a two-photon absorption dominates at a shorter wavelength.

Conclusions

The fluorogenic probes for redox metabolism, 1–6, show two-photon absorption using the pulses of a femtosecond Ti/

TABLE 1: Two-Photon Absorption Cross Sections (δ) and Fluorescence Quantum Yields (Φ_f)

	absorption method	fluorescence method		Φ_f^c
	δ (GM) ^{ab} @ 775 nm	δ (GM) ^{ab} @ 775 nm	δ (GM) ^{ab} @ λ_{\max}	
1	2.9			<0.001
2	3.8	8.0	8.9 (800 nm) ^d	0.65
3	5.8	9.0	9.6 (750 nm) ^d	0.86
4	<1 ^f	0.023	0.11 (750 nm) ^d	0.41
5	7.1 ^g	2.2 ^g	4.0 ^g (750 nm) ^d	0.04 ^g
6	<1 ^f	0.002	0.041 (730 nm) ^e	0.21

^a GM: Goepfert-Mayer units (1 GM = 10^{-50} cm⁴ s photon⁻¹).

^b Error limit 20%. ^c Error limit 10%. ^d Maximum of two-photon absorption spectrum. ^e Shortest wavelength measured. The maximum of the two-photon absorption is probably below 730 nm. ^f Too small to be determined. ^g Error limit ~ 30%.

sapphire laser. Excellent contrast ratios between the fluorescence of the alcohol versus that of the ketone derivatives were observed: 290:1 (**2:1**), 1:180 (**4:3**), and 1:200 (**6:5**) which are dramatically enhanced in comparison with those obtained in standard one-photon excitation. In the context of metabolic imaging, this finding may translate to achieving superior detection limits of probe conversion (e.g., low activity pathways) with two-photon fluorescence microscopy. Furthermore, this work provides new guidelines for the design of resonance-based optical switches operating in a two-photon regime.

The practical applicability of the two-photon-excitation redox switch, **1** and **2**, was demonstrated in an enzyme-catalyzed process. The nonfluorescent probe **1** is efficiently converted by AKR1C3, a 3 α -HSD, to the fluorescent derivative **2**. The conversion kinetics was monitored by fluorescence of **2** after two-photon excitation using NIR laser pulses (775 nm). A large contrast ratio between the fluorescence in the presence and that in the absence of the enzyme of ~300 was achieved. This high contrast ratio together with the advantages of two-photon excitation should make this reported probe very attractive for 3 α -HSD detection.

Acknowledgment. N.J.T. and S.J. are thankful for financial support by the Center of Excellence in Genomic Science Grant P50 HG002806 from the National Institutes of Health and by

NSF CHE-04-15516. D.J.Y. acknowledges the ACS Division of Medical Chemistry and Wyeth Research for a predoctoral fellowship. D.S. thanks the G. Harold and Leila Y. Mathers Charitable Foundation. The work at Buffalo was supported by the directorate of chemistry and life science of the Air Force office of Science Research.

Supporting Information Available: UV-vis absorption spectra (one-photon absorption), extinction coefficients, and fluorescence lifetimes for **1–6**. This material is available free of charge via the Internet at <http://pubs.acs.org>.

References and Notes

- Weissleder, R.; Ntziachristos, V. *Nat. Med.* **2003**, *9*, 123.
- Moreira, R.; Havranek, M.; Sames, D. *J. Am. Chem. Soc.* **2001**, *123*, 3927.
- Chen, C.-A.; Yeh, R.-H.; Lawrence, D. S. *J. Am. Chem. Soc.* **2002**, *124*, 3840.
- Boonacker, E.; Van Noorden, C. J. F. *J. Histochem. Cytochem.* **2001**, *49*, 1473.
- Handbook of Fluorescent Probes and Research Chemicals, Molecular Probes*, 9th ed.; Haugland, R. P., Ed.; Molecular Probes: Eugene, OR, 2002.
- Yee, D. J.; Balsanek, V.; Sames, D. *J. Am. Chem. Soc.* **2004**, *126*, 2282.
- Yee, D. J.; Balsanek, V.; Bauman, D. R.; Penning, T. M.; Sames, D. *Proc. Natl. Acad. Sci. U.S.A.* **2006**, *103*, 13304.
- Lakowicz, J. R. *Nonlinear and two-photon-induced fluorescence spectroscopy. Topics in Fluorescence Spectroscopy*; Plenum Press: New York, 1997; Vol. 5.
- Prasad, P. N. *Introduction to Biophotonics*; Wiley: New York, 2003.
- Belfield, K. D.; Liu, Y.; Liu, J.; Ren, X.; Van Stryland, E. W. *J. Phys. Org. Chem.* **2000**, *13*, 837.
- Morris, J. V.; Mahaney, M. A.; Huber, J. R. *J. Phys. Chem.* **1979**, *80*, 969.
- He, G. S.; Xu, G. C.; Prasad, P. N.; Reinhardt, B. A.; Bhatt, J. C.; Dillard, A. G. *Opt. Lett.* **1995**, *20*, 435.
- He, G. S.; Lin, T.-C.; Dai, J.; Prasad, P. N.; Kannan, R.; Dombroskie, A. G.; Vaia, R. A.; Tan, L.-S. *J. Chem. Phys.* **2004**, *120*, 5275.
- Albota, M. A.; Xu, C.; Webb, W. W. *Appl. Opt.* **1998**, *37*, 7352.
- Xu, C.; Webb, W. W. *J. Opt. Soc. Am. B* **1996**, *13*, 481.
- Penning, T. M.; Burczynski, M. E.; Jez, J. M.; Hung, C.-F.; Lin, H.-K.; Ma, H.; Moore, M.; Palackal, N.; Ratnam, K. *Biochem. J.* **2000**, *351*, 67.
- Wakebe, T.; Van Keuren, E. *Jpn. J. Appl. Phys.* **1999**, *38*, 3556.
- Chen, G.; Yee, D. J.; Gubernator, N.; Sames, D. U.S. Patent WO2006026368, 2006.
- Yee, D. J.; Balsanek, V.; Sames, D., U.S. Patent WO2006023821, 2006.